Preparation and Conductive Properties of Polycaprolactone-Grafted Carbon Black Nanocomposites

Jianguo Cheng,[1,2] Li Wang,[1] Jia Huo,[1] Haojie Yu,[1] Qiang Yang,[1] Libo Deng[1]

[1]*Department of Chemical and Biological Engineering, The State Key Laboratory of Chemical Engineering, Zhejiang University, Hangzhou 310027, People's Republic of China*
[2]*Department of Chemical Engineering, Hangzhou Vocational and Technical College, Hangzhou 310018, People's Republic of China*

Received 1 May 2008; accepted 8 March 2009
DOI 10.1002/app.30569
Published online 16 July 2009 in Wiley InterScience (www.interscience.wiley.com).

ABSTRACT: Polycaprolactone-grafted carbon black (CB-*g*-PCL) nanocomposites were prepared by surface-initiated ring-opening polymerization of ε-caprolactone on the surface of CB. Thermogravimetric analysis (TGA), differential scanning calorimetry (DSC), atomic force microscope (AFM), X-ray diffraction (XRD), and polarizing optical microscope (POM) method were employed to characterize the resultant CB-*g*-PCL. The effect of temperature on resistivity of polycaprolactone-grafted CB (CB-*g*-PCL) nanocomposites was investigated and compared with that of mixture of CB and PCL. It was found that CB-*g*-PCL nanocomposites exhibited positive temperature coefficient (PTC) phenomena between 48 and 51°C, and negative temperature coefficient (NTC) phenomena and between 51 and 54°C. The prepared CB-*g*-PCL nanocomposites have the potential to be temperature-dependent switch materials. © 2009 Wiley Periodicals, Inc. J Appl Polym Sci 114: 2700–2705, 2009

Key words: polycaprolactone; grafted carbon black; conductivity; PTC; NTC

INTRODUCTION

Recently, polymer composites showing change of resistivity with temperature have attracted much attention, which could be applied to various areas, such as functional dielectric materials,[1] smart materials,[2] and so on.[3,4] Various conductive particles, such as carbon black (CB), carbon nanotubes, carbon fibers or metal particles, have been added into polymer matrix to prepare these materials. Compared with carbon nanotubes, carbon fibers or metal particles, CB shows the desirable conductive properties, and has abundant sources and inexpensive cost, despite without ordered structures.[4–6] These composites were often prepared by physical blend of conductive particles and polymers, which possibly resulted in inhomogeneous dispersion of particles, incompatibility with the matrix, and thus relatively temporary stability and short life-span of the resultant materials.[4–8] For example, Hindermann-Bischoff and Ehrburger-Dolle[3] reported a kind of polyethylene/CB composite displaying obvious positive temperature coefficient (PTC) phenomenon, but the PTC intensity and stability of the composites were relatively weak due to the aggregate of CB. Xu and Dang[7] prepared four systems of conductive filler (CB, Ni, Zn, and W)/polyvinylidene fluoride (PVDF) composites, which exhibited PTC effect. However, the content of fillers at percolation was higher than other systems, because the fillers always aggregated in the amorphous phases. These problems are expected to be circumvented by introducing polymers on the surface of inorganic particles, which would improve the dispersibility and compatibility of particles with the polymer matrixes, and thus the PTC stability of the resultant.

Many methods have been utilized to prepare polymer-grafted carbon nanomaterials,[9–19] such as anion,[12] cation,[13] and surface-initiated[14] ring-opening polymerization. Recently, we also reported the preparation of PCL-grafted CB nanoparticles by surface-initiated ring-opening polymerization of ε-caprolactone,[15,16] and found surface-initiated ring-opening polymerization was one of convenient and efficient approaches to prepare core-shell CB nanocomposites. In addition, it is expected that CB-*g*-PCL can disperse homogenously in the polymer matrix and exhibit interesting temperature-dependent conductive property. As a result, here, we prepared the polycaprolactone-grafted CB (CB-*g*-PCL) nanocomposites and investigated the effect of temperature on resistance of the CB-*g*-PCL. To compare the influence of grafted PCL on electrical property of the CB-*g*-PCL, the conductive property of mixtures of CB and PCL were studied as well.

Correspondence to: L. Wang (opl_wl@dial.zju.edu.cn).

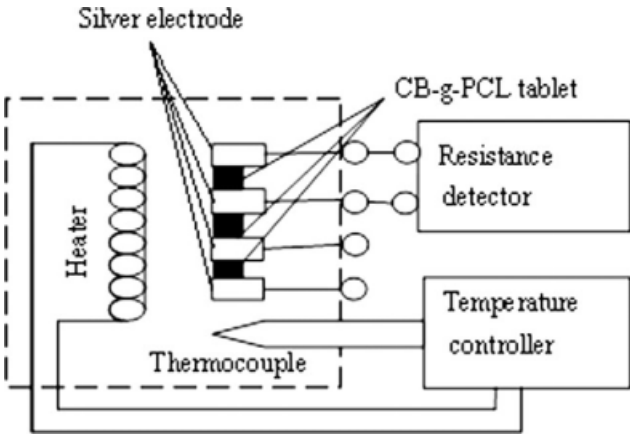

Figure 1 The equipment for temperature/resistivity detection.[14]

EXPERIMENTAL SECTION

Materials

Primary CB particles (VXC 605) with an average diameter of 30 nm and a specific area of 254 m^2/g were obtained from Cabot Co. ε-caprolactone and stannous ocatoate ($Sn(Oct)_2$) were purchased from Acros. Hydroxyl grafted CB (CB—OH) was prepared according to the literature[15]. Other solvents and reagents were at least analytical grade.

Preparation of polycaprolactone-grafted carbon black (CB-*g*-PCL) nanocomposites and mixture of CB and PCL

CB-*g*-PCL nanocomposites were prepared according to the literature.[15] A typical method to prepare was as follow: CB—OH (0.10 g, 0.14 mmol —OH) was treated with $Sn(Oct)_2$ (4.05 mg, 10 μmol) in 16 mL of dried toluene for 1 h at 55°C under Ar protection. ε-caprolactone (4 mL, 37.5 mmol) was then added with a syringe and the mixture was heated at 100°C for 24 h. CB-*g*-PCL was obtained by centrifugation in THF for three times and then dried at 50°C in vaccum for 24 h. The content of PCL grafted on the surface of CB can be controlled by changing the amount of PCL or the reaction time.

Mixture of CB and PCL was prepared as a comparison. In order to improve the dispersity of CB in PCL, 0.54 g CB was added into PCL solution with 0.46 g PCL in 10 mL THF, then the suspension was treated with ultrasonic waves for 30 min and finally dried in vacuum at 50°C for 24 h. The content of PCL in the mixture can be changed by tuning the weight ratio of PCL and CB.

Characterization

TGA was carried out on a Perkin-Elmer TGA-7 instrument with a heating rate of 20°C/min, from 25°C to 800°C in a flow of nitrogen. Melting point temperature (T_m) was recorded on a Perkin-Elmer DSC-7 differential scanning calorimeter (DSC) at a heating rate of 20°C/min. XRD spectrum was recorded on a Rigaku-D/max-Ra (Cu K_a, $\lambda = 1.54$Å). POM images were obtained from NIKON ECLIPSE E600POL. AFM measurements were carried out on SPA 400 (Seiko instrument Inc) in tapping mode with a J scanner.

Measurement of conductive property of CB-*g*-PCL and mixture of CB and PCL

The conductive property of the CB-*g*-PCL flake at different temperature was measured by homemade equipment shown in Figure 1. First, a flake of sample was produced as follows: 0.72 g of the CB-*g*-PCL powders were added into a tablet pressing machine to form a round tablet with a thickness of 0.36 cm under 30 atm; then the tablet was sandwiched between two silver electrodes after hand-polished to a mirror finish; finally, the relationship between resistivity and temperature of sample was recorded with a 9932FC multimeter at different temperatures. The testing method of the conductive property of the mixture of CB and PCL was the same with that of CB-*g*-PCL, except the CB-*g*-PCL tablet was replaced by the tablet of mixture of CB and PCL.

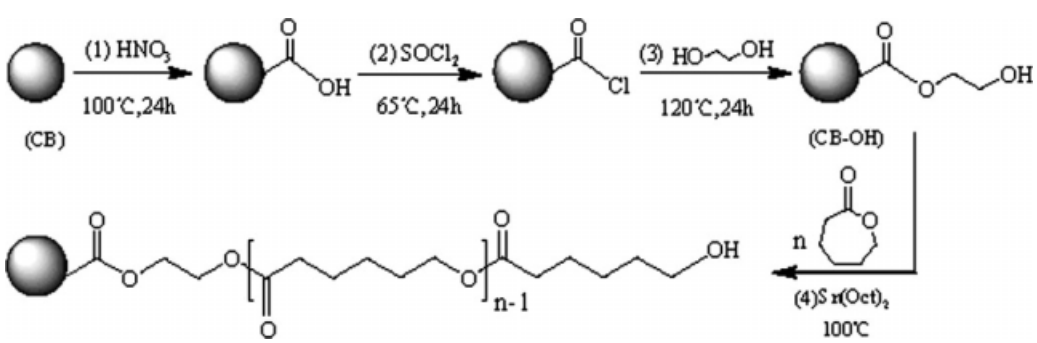

Figure 2 The preparation route of CB-*g*-PCL.[15]

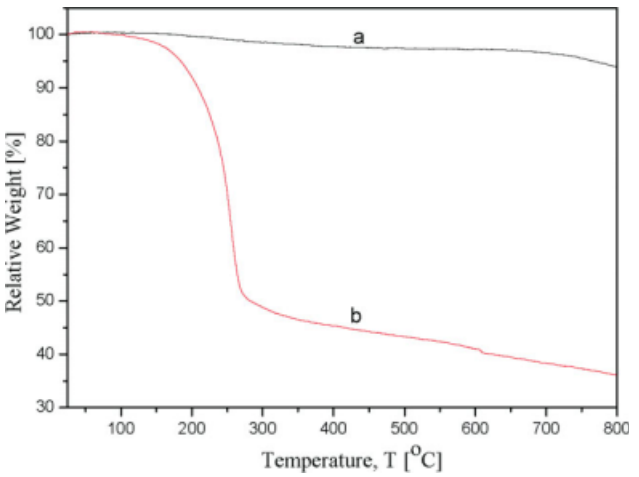

Figure 3 TGA curves of pure CB (a) and CB-*g*-PCL (b).[20] [Color figure can be viewed in the online issue, which is available at www.interscience.wiley.com.]

RESULTS AND DISCUSSION

Preparation, morphology, thermal behavior, and crystallization analysis of CB-*g*-PCL

It was reported that surface-initiated ring-opening polymerization of ε-caprolactone was an effective method to prepare core-shell structure nanoparticles.[15] We employed this method to introduce PCL onto the surface of CB. Figure 2 illustrates the synthetic approach, which has been shown in our previous work.[15] The content of PCL in CB-*g*-PCL was about 51.9%, calculated from TGA data (Fig. 3), by comparing the thermal weight loss of pure CB and CB-*g*-PCL between 25 and 300°C.[15]

AFM was employed to characterize the morphology of CB-*g*-PCL. AFM image showed that the resultant CB-*g*-PCL formed isolated spherical assembly with average diameter of approximate 200 nm, without apparent aggregation (Fig. 4). The spherical assembly is a core-shell structure with CB as the "core" and PCL layer as the shell.

XRD was used to certify the formation of core-shell structure of CB-*g*-PCL. XRD spectrum of CB-*g*-PCL is shown in Figure 5(a), and the diffraction peaks at 16.5°, 17.1°, and 18.7° in Figure 5(a) are the characteristic peaks of PCL,[21] indicating the CB was wrapped by the PCL, which is consistent with the result from AFM. The crystallization behavior of CB-*g*-PCL was studied by DSC as shown in Figure 5(b) and an obvious endothermal peak can be observed at 51°C. As the CB particle do not show any phase transition in the range of testing temperatures, this peak results from melting of PCL, which is also close to the melting point of pure PCL.[22]

The crystallization behavior of CB-*g*-PCL and pure PCL was further characterized by POM (Fig. 6). It is found that the spherical crystal of CB-*g*-PCL is relative smaller with a blurry interface.[21] The reason may be that the CB particles play as nucleation agents for PCL after polymerization of CL on the surface of CB. As the amount of nucleation agent increased, the crystal growing rate increased, and thus the spherical crystal became smaller.[23–25]

Conductive property of CB-*g*-PCL and conductive mechanism

Then, we investigated the effect of temperature on resistance of CB-*g*-PCL with different contents of PCL (19.6%, 40.6%, and 51.9%), shown in Figure 7. It is found that CB-*g*-PCL nanocomposites exhibit clear PTC phenomenon between 48 and 51°C and NTC phenomenon between 51 and 54°C (Fig. 7), except for CB-*g*-PCL with 19.6% of PCL. Many theories have been employed to explain the PTC phenomenon for different kinds of conductive polymers.[26–31] In this case, the change of resistance

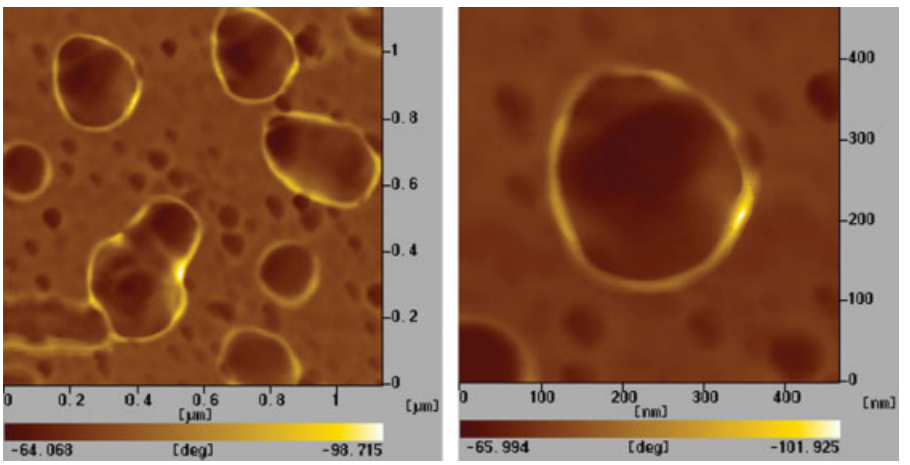

Figure 4 AFM images of CB-*g*-PCL. [Color figure can be viewed in the online issue, which is available at www.interscience.wiley.com.]

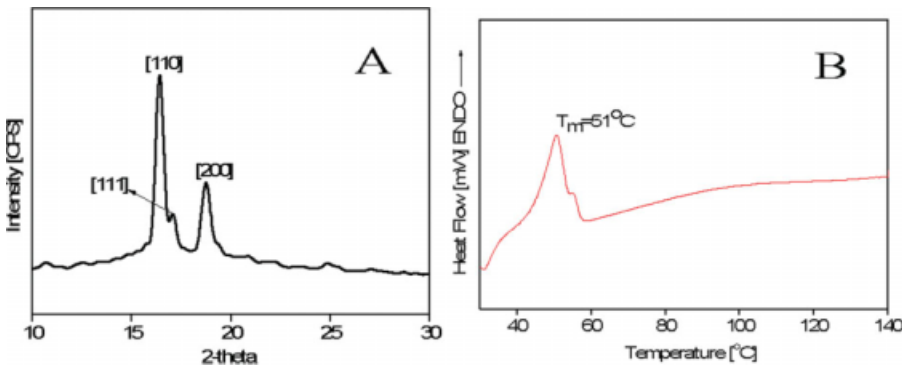

Figure 5 XRD spectrum (a) and DSC curve (b) of CB-*g*-PCL. [Color figure can be viewed in the online issue, which is available at www.interscience.wiley.com.]

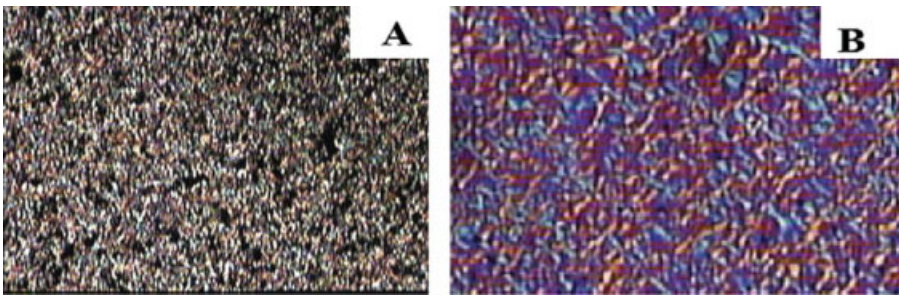

Figure 6 POM images of CB-*g*-PCL (a) and PCL (b). [Color figure can be viewed in the online issue, which is available at www.interscience.wiley.com.]

experienced three processes with the increasingly temperature, which possibly resulted from the gradual phase transfer of the polymer crystal induced by temperature. The proposed mechanism is shown in Figure 8. When the temperature is below melting point ($T < 48$°C), the polymer swells slightly and thus the distance between the individual CB particles has a little change, which is reflected by the unconspicious variation of resistance in the temperature region 25–48°C. With the temperature approaching the melting point of polymer crystal, the expand coefficient of CB-*g*-PCL nanoparticle reaches its maximum, the nanoparticle swells remarkably, and thus the resistance of CB-*g*-PCL increases sharply, which is the typical characteristic of PTC effect (48–51°C). When the temperature is over than the melting point, the softened CB-*g*-PCL nanoparticle begins to flow and the CB particle redistributes in the system, making the conductive channel increased. Hence, it is reasonable that the CB-*g*-PCL nanoparticle exhibites NTC phenomenon when the temperature is between 51 and 54°C. It is noted that the change of resistance with the temperature is a reversible process, that is, the resistance can recover to its initial value when the temperature decreases to 25°C [Fig. 9(a)]. As for CB-*g*-PCL with lower content of PCL (19.6%), the expansion of nanoparticle is not obvious so that the resistivity do not show apparent change.

The melting point and the time kept at melting point would influence the micro-ordered region, which possibly exists in the polymer and the crystal

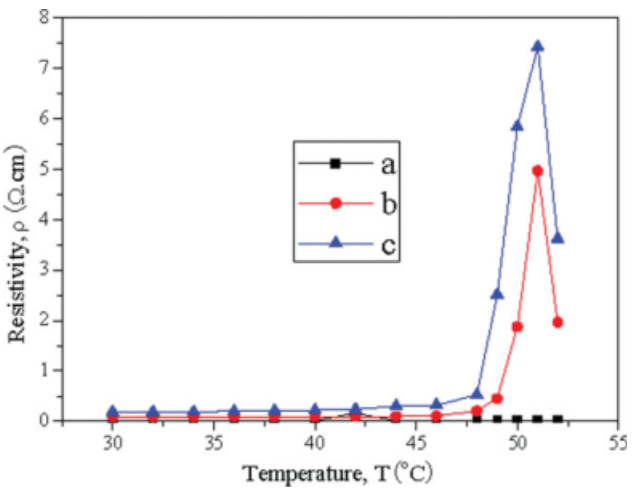

Figure 7 Dependence of resistivity of CB-*g*-PCL on PCL content: (a) 19.6%; (b) 40.6%; (c) 51.9%. [Color figure can be viewed in the online issue, which is available at www.interscience.wiley.com.]

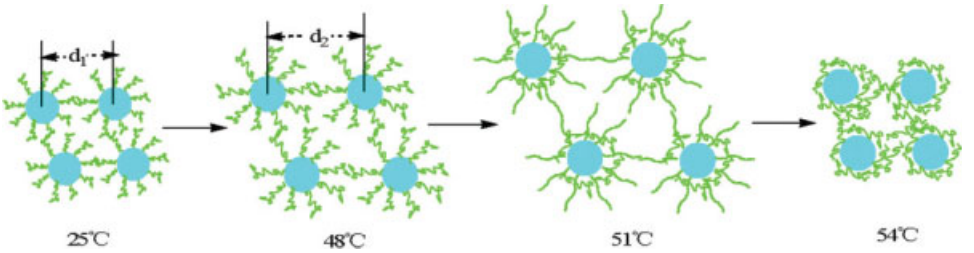

Figure 8 Possible mechanisms for PTC and NTC phenomenon formation of CB-*g*-PCL at different temperatures. [Color figure can be viewed in the online issue, which is available at www.interscience.wiley.com.]

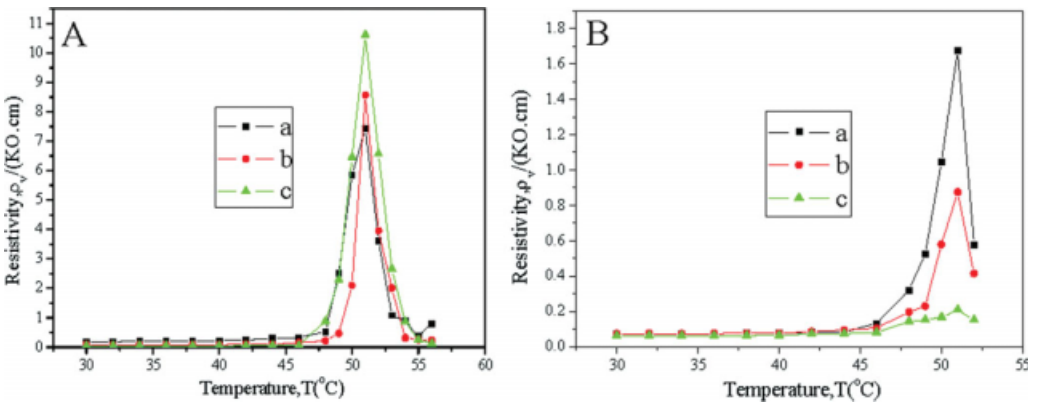

Figure 9 Dependence of resistivity of CB-*g*-PCL (A) and mixture of CB and PCL (B) on temperature: (a) first; (b) second; (c) third measurement. [Color figure can be viewed in the online issue, which is available at www.interscience.wiley.com.]

nucleus as well, and temperature is also one of the most important factors that affect the crystallization process of polymers. Generally, the polymer crystals are destroyed more seriously and the residual crystal nucleus decreases at higher temperature; at lower temperature, the crystal nucleus in the system would induce heterogeneous crystal nucleation and therefore speed up the crystal process and decrease the crystal size along with the size distribution.

We also investigated the reproducibility and stability of the behavior of temperature-responsive resistance, and compared these properties of CB-*g*-PCL with blended mixture of CB and PCL (Fig. 9). As the CB nanocomposite with 51.9% PCL exhibits excellent PTC and NTC effects, this system was selected to study the reproducibility and stability of the behavior of temperature-responsive resistance. For the blended mixture, the PTC plots exhibit remarkable difference in multiple thermal cycles, i.e., the electrical property is unstable. The reason may be that, the interaction between CB particle and the nonpolar PCL is very weak, and then CB particles tend strongly to assemble together. However, for CB-*g*-PCL, the reproducibility and stability of the behavior of temperature-responsive resistance (Fig. 9) are much better than those of the blended mixtures. This is presumably due to the stronger interaction between CB and PCL.

CONCLUSIONS

Summarily, CB-*g*-PCL nanocomposites were prepared by surface-initiated ring-opening polymerization of ε-caprolactone on the surface of CB. DSC, AFM, XRD, and POM method were employed to investigate the resultant CB-*g*-PCL. CB-*g*-PCL nanoparticle containing 51.99% CB exhibited obvious PTC phenomenon between 48 and 51°C, and NTC phenomenon between 51 and 54°C, respectively. By a comparison with the resistance-temperature behavior of blended mixture of CB and PCL, it was found that the introduction of PCL onto CB surface resulted in PTC/NTC phenomenon for CB-*g*-PCL. The prepared CB-*g*-PCL nanocomposites can be used as the temperature-dependent switch materials.

References

1. Xu, H. P.; Dang, Z. M.; Yao, S. H.; Jiang, M. J.; Wang, D. Y. Appl Phys Lett 2007, 90, 152912.
2. Wan, Y.; Wen, D. J. Smart Mater Struct 2005, 14, 941.
3. Hindermann-Bischoff, M.; Ehrburger-Dolle, F. Carbon 2001, 39, 375.
4. Chen, S. G.; Hu, J. W.; Zhang, M. Q.; Li, M. W.; Rong, M. Z. Carbon 2004, 42, 645.
5. Sun, Z. X. Electronic Chemicals; Chemical Industry Press: Beijing, 2001.
6. Briguglio, J. J.; Keil, C. R.; Taravinal, M.; Reardon, E. J. J.; Kautz, R. W.U.S. Pat. 5609991 (1997).

7. Xu, H. P.; Dang, Z. M. Chem Phys Lett 2007, 438, 196.
8. Bin, Y.; Xu, C.; Zhu, D.; Matsuo, M. Carbon 2002, 40, 195.
9. Yuen, S. M.; Ma, C. C.; Chiang, C. L.; Lin, Y. Y.; Teng, C. C. J Polym Sci Part A: Polym Chem 2007, 45, 3349.
10. Reddy, K. R.; Lee, K. P.; Gopalan, A. I.; Kim, M. S.; Showkat, A. M.; Nho, Y. C. J Polym Sci Part A: Polym Chem 2006, 44, 3355.
11. Wu, T. M.; Lin, S. H. J Polym Sci Part A: Polym Chem 2006, 44, 6449.
12. Tsubokawa, N. J Macromol Sci Chem 1987, 24, 763.
13. Tsubokawa, N.; Jian, Y.; Sone, Y. J Polym Sci Part A: Polym Chem 1988, 26, 2715.
14. Cheng, J. G.; Wang, L.; Huo, J.; Yu, H. J.; Yang, Q.; Deng, L. B. J Polym Sci Part B: Polym Phys 2008, 46, 1529.
15. Yang, Q.; Wang, L.; Xiang, W. D.; Zhou, J. F.; Deng, L. B.; Li, J. H. Eur Polym J 2007, 43, 1718.
16. Yang, Q.; Wang, L.; Xiang, W. D.; Zhou, J. F.; Tian, J. H. J Polym Sci Part A: Polym Chem 2007, 45, 3444.
17. Yang, Q.; Wang, L.; Xiang, W. D.; Zhou, J. F.; Li, J. H. Polymer 2007, 48, 2866.
18. Yang, Q.; Wang, L.; Xiang, W. D.; Zhou, J. F.; Jiang, G. H. J Appl Polym Sci 2007, 103, 2086.
19. Yang, Q.; Wang, L.; Xiang, W. D.; Zhou, J. F.; Tan, Q. H. Polymer 2007, 48, 3444.
20. Wu, T. M.; Chen, E. C. J Polym Sci Part B: Polym Phys 2006, 44, 598.
21. Yoshii, F.; Darwis, D.; Mitomo, H.; Makuuchi, K. Radiat Phys Chem 2000, 57, 417.
22. Kožíšek, Z.; Hikosaka, M.; Demo, P.; Sveshnikov, A. M. J Cryst Growth 2005, 275, E79.
23. Xu, T.; Lei, H.; Xie, C. S. Mater Des 2003, 24, 227.
24. He, J. M.; Chen, W. X.; Dong, X. X. Physics of Polymer; Press of Fudan University: Shanghai, 2000.
25. Menges, G.; Thienel, P. Polym Eng Sci 1977, 17, 758.
26. Ohe, K.; Natio, Y. Jpn J Appl Phys 1971, 10, 99.
27. Klason, C.; Kubat, J. J Appl Polym Sci 1978, 19, 831.
28. Allak, H. M.; Brinkman, A. W.; Woods, J. J Mater Sci 1993, 28, 117.
29. Shen, L.; Xu, J. W.; Yi, X. S. Acta Mater Compos Sin 2001, 18, 34.
30. Blaszkiewicz, M.; Mclachlan, D. S.; Newnhan, R. E. Polym Eng Sci 1992, 32, 421.
31. Yang, Q. Ph.D. Thesis, Zhejiang University, 2007.